Asian Journal of Chemistry; Vol. 38, No. 1 (2026), 75-81
ASIAN JOURNAL OF CHEMISTRY
https://doi.org/10.14233/ajchem.2026.34812

Novel Functional Acrylic Copolymers: Synthesis, Characterization, Molecular Docking and Biological Efficacy

RAJESH J. PATEL[1,*], BINDU C. PATEL[2], AKASH K. PATEL[1], RITESH R. CHAUHAN[1], ZARNA R. PATEL[3], JATIN D. PATEL[3], PRITESH M. THAKOR[3], KEYUR M. PANDYA[4] and CHIRAG R. PATEL[5]

[1]Department of Chemistry, Sardar Patel University, Vallabh Vidyanagar-388120, India
[2]Department of Chemistry, Shri M.B. Patel Science College, Anand-388001, India
[3]Department of Chemistry, Shri Alpesh N. Patel Post Graduate Institute of Science and Research, Anand-388001, India
[4]Department of Chemistry, Veer Narmad South Gujarat University, Surat-395007, India
[5]Department of Chemical Engineering, Dharmsinh Desai University, Nadiad-387003, India

*Corresponding author: E-mail: dr.rjpatel_07@spuvvn.edu

Received: 1 September 2025 *Accepted*: 5 November 2025 *Published online*: 31 December 2025 AJC-22224

In this study, the functional methacrylate monomers 2,4-dichlorophenyl methacrylate (2,4-DMA) and vanillin methacrylate (VMA) were synthesized and subjected to free-radical (co)polymerization at controlled feed ratios to generate a compositionally tunable copolymer series. Monomer-to-polymer conversion and chain microstructure were verified using FT-IR, ^{1}H NMR and HPLC. The disappearance of vinyl proton resonances and the loss of C=C stretching bands, combined with high chromatographic purity (>99%), confirmed efficient propagation and minimal side reactions. Compositional variations in the copolymers were further reflected in systematic shifts in carbonyl and aromatic vibrational domains, consistent with differing contributions of the 2,4-dichlorophenyl and vanillin units to the polymer backbone. Biological evaluation demonstrated a clear composition-dependent antimicrobial response, with 2,4-DMA-rich copolymers exhibiting the highest inhibition against both bacterial and fungal strains. To complement the experimental findings, a molecular docking analysis was also performed against *E. coli* DNA gyrase (PDB: 1KZN). The selected copolymer fragment displayed a binding affinity of –5.20 kcal/mol, supported by hydrogen bonding with ASN46 and stabilizing π-alkyl, π-sigma, and alkyl interactions with residues such as ALA47, THR165, VAL43 and VAL167, consistent with the observed antibacterial potency. Based on the results, this study establishes 2,4-DMA/VMA copolymers as a structurally adaptable platform with tunable antimicrobial performance enhanced by favorable protein-binding interactions. These materials show promising aspects for antimicrobial coatings, protective films and biologically responsive polymer systems.

Keywords: Acrylic copolymers, 2,4-Dichlorophenyl methacrylate, Vanillin methacrylate, Docking studies, Antimicrobial activity.

INTRODUCTION

Acrylic polymers continue to occupy a central position in modern materials science due to their tunable structural features and broad application range. Among them, phenyl acrylate based polymers have emerged as an important class of functional materials, gaining increasing attention compared to long-established commercial polymers such as vinyl derivatives, acrylamides and alkyl acrylates [1,2]. Their homopolymers and copolymers exhibit prominent versatility, enabling their adoption across diverse industrial sectors including films, fibers, protective coatings, lithographic systems, lacquers, adhesives, printing inks and binder formulations [3,4].

The high reactivity of phenyl acrylates originates from the presence of an aromatic ring within their molecular architecture, imparting unique electronic and steric attributes during polymerization. Among these, chlorinated phenyl methacrylate derivatives and their corresponding polymers have attracted growing scientific interest due to their structural diversity and functional adaptability across multiple domains [5,6]. For instance, copolymers derived from chlorophenyl acrylate and methacrylate have been successfully utilized as base coatings in leather processing, demonstrating their suitability for specialized surface-engineering applications [7].

The industrial success of methacrylate polymers is also linked to their capacity to be precisely tailored for rigid-use

applications, where properties such as mechanical stability, optical clarity, dimensional retention and resistance to environmental degradation are essential. This high degree of tunability has supported their extensive adoption in technologically demanding sectors. In construction materials, incorporation of acrylate monomers into cementitious composites has been shown to significantly improve the intrinsic brittleness and limited flexural strength of conventional cement-based systems [8]. In advanced photonic applications, methacrylate templates such as poly(methyl methacrylate) (PMMA) have enabled the development of ultrafast non-linear optical devices, including high-performance optical phase–frequency synthesizers [9]. In biomedical engineering, the incorporation of bifunctional monomers with hydrophilic and hydrophobic domains has improved adhesion and anti-bacterial performance in dental and medical-grade polymers [10]. Furthermore, acrylic-based formulations contribute significantly to solar energy conservation systems, where they function as stable protective coatings for reflective substrates [11].

Acrylic polymers also demonstrate remarkable functionality in non-rigid and flexible polymeric systems. Cyanoacrylate-modified methacrylates remain widely used in high strength adhesive formulations compatible with metals, ceramics, glass and several engineering plastics [12]. In lubrication technology, long-chain polymethacrylates serve as effective viscosity modifiers and multifunctional additives, improving low-temperature performance, dispersion stability and oxidetive resistance in lubricants [13-16]. Acrylic dispersions and solution polymers also support multi-coat deposition technologies used across wood finishing, metal fabrication, can coating and coil coating applications [17-22]. In the textile sector, acrylic polymers contribute to smart fabric development, enhancing soil repellency, durability and other functional attributes without compromising tactile properties [23-26].

Based on the growing importance of phenyl acrylate-based polymers across both rigid and flexible material platforms, the development of structurally tunable derivatives with enhanced biological activity represents a promising research frontier. In this context, the present study focuses on the synthesis, characterization and biological evaluation of functional methacrylate copolymers designed to combine chemical reactivity with antimicrobial potential.

EXPERIMENTAL

The chemicals and solvents including methacrylic acid, benzoyl chloride (TCI Pvt. Ltd., India), hydroquinone (Loba Chemie Pvt. Ltd., India), 2,4-dichlorophenol, toluene (SRL Pvt. Ltd., India), sodium hydroxide, *N*,*N*-dimethylformamide (DMF, Sisco Chem Pvt. Ltd., India), azobisisobutyronitrile (AIBN, A.B. Enterprises, India), vanillin (Samir Tech-Chem Pvt. Ltd., India) and ethanol were of analytical grade with minimum purity of 98%.

General procedure for synthesis of functional copolymers

(i) Synthesis of methacryloyl chloride (MC): Anhydrous methacryloyl chloride (MC) was synthesized according to a literature method [27]. In brief, methacrylic acid (1.0 mol) was reacted with benzoyl chloride (2.0 mol) in the presence of hydroquinone (0.0025 mol) as a polymerization inhibitor. The reaction mixture was distilled and the crude product was further purified by redistillation to yield colourless MC (b.p. 95-96 ºC, yield: ~85%).

(ii) Synthesis of 2,4-dichlorophenyl methacrylate (2,4-DMA): Firstly, NaOH (0.2 mol) was dissolved in ethanol, followed by addition of 2,4-dichlorophenol to form the corresponding phenoxide. The mixture was heated at 60 ºC for 30 min and subsequently cooled to 0-5 ºC. Freshly distilled MC (0.21 mol) was added dropwise over 90 min. The reaction mixture was poured into ice-cold water, leading to precipitation of the product. The solid was collected by vacuum filtration, washed with cold water and dried to afford pure 2,4-DMA.

(iii) Synthesis of vanillin methacrylate (VMA): Vanillin was converted to its alkoxide by adding it to a chilled ethanolic NaOH solution (3.0 g in 200 mL ethanol). After cooling to 0-5 ºC, MC was added dropwise over 2-3 h. The reaction was quenched by pouring into ice-water, resulting in the precipitation of VMA, which was isolated by filtration and dried.

(iv) Homopolymerization of 2,4-DMA and VMA: Homopolymers were synthesized *via* free-radical polymerization in toluene using AIBN as the initiator. Each monomer solution was maintained at 70 ºC until polymerization process was complete. Then, the resulting polymers were isolated and dried.

(v) Copolymerization of 2,4-DMA and VMA: Radical initiated copolymerization was carried out by mixing defined amounts of 2,4-DMA, VMA, AIBN and toluene in a reaction tube. Polymerization was conducted at 70 ºC under stirring and terminated at low conversion (< 10%) to satisfy the copolymerization equation. The solution was cooled and precipitated in excess methanol (**Scheme-I**). The obtained copolymers were purified by repeated dissolution in DMF followed by reprecipitation in methanol and dried to constant weight.

Characterization: The polymeric samples were characterized by utilizing FT-IR spectra (Nicolet 400D) using KBr pellets. The ^{1}H NMR spectra were recorded on a 60 MHz Hitachi-R-1500 spectrometer using deuterated chloroform ($CDCl_3$) as solvent and tetramethylsilane (TMS) as internal standard. Monomer purity for 2,4-DMA was determined by HPLC on a Waters system equipped with a 510 pump, a μ-Bonda Pak C_{18} column and a 486-absorbance detector. The analysis was performed with methanol as the mobile phase, injecting 20 μL of 0.5 mg/mL sample solution.

Biocidal potency: The antimicrobial efficacy of acrylic copolymers against selected bacterial and fungal strains in a systematical manner. All microbial cultures (*Enterococcus faecium*, *Bacillus megaterium*, *Escherichia coli*, *Salmonella* spp., *Aspergillus niger*) maintained on enriched nutrient were procured from the Department of Biosciences at Sardar Patel University. The growth inhibition assays were conducted using established protocols with a standardized copolymer concentration [28]. In brief, a culture (5-10% v/v) inoculum was aseptically transferred to both control (polymer-free) and polymer-amended (50 mg/100 mL) N-broth. The cultures were incubated at 28 ± 2 ºC with continuous agitation at 200 rpm for 40 h. At regular intervals, 0.5 mL aliquots were withdrawn, appropriately diluted and the cell growth was quantified by measuring the optical density at 660 nm (OD_{660}/mL). The inhibition percentage were derived from:

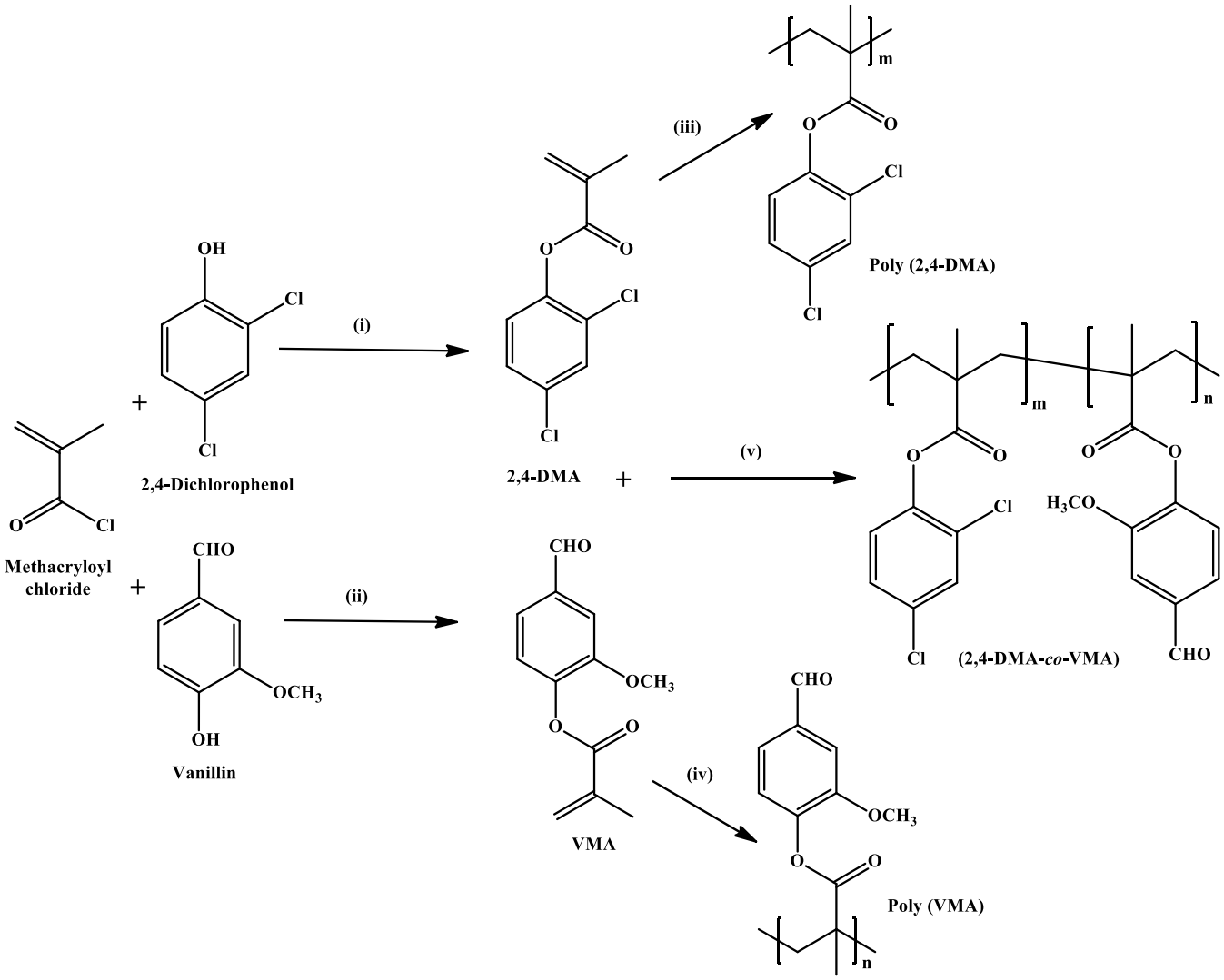

Scheme-I: Synthesis of 2,4-DMA, VMA, poly (2,4-DMA), poly (VMA) & (2,4-DMA-co-VMA). (i) NaOH, Ethanol, 0-5 ºC (ii) NaOH, ethanol, 0-5 ºC (iii) toluene, AIBN, 70 ºC (iv) DMF, AIBN, 70 ºC and (v) toluene, AIBN, 70 ºC

$$\text{Inhibition (\%)} = \frac{(X-Y)}{X} \times 100$$

where X = OD_{660} of control culture and Y = OD_{660} of test culture.

Docking studies: Molecular docking was performed to evaluate the interaction of the methacrylate-based copolymer with bacterial DNA gyrase. The crystallographic structure of DNA gyrase (PDB ID: 1KZN) was retrieved from the Protein Data Bank and prepared by removing co-crystallized ligands, water molecules and adding polar hydrogens. The ligand structure was energy-minimized prior to docking. Docking simulations were carried out using standard protocols [29,30] and the resulting binding poses were ranked based on binding affinity values. The compound selected for the docking corresponded to the copolymer component that exhibited the highest antibacterial activity *in vitro*.

RESULTS AND DISCUSSION

The newly synthesized 2,4-DMA and VMA monomers were polymerized and copolymerized at various feed ratios. Table-1 shows that under low-conversion radical copolymerization, increasing the mole fraction of 2,4-DMA in the feed leads to a corresponding increase in its incorporation within the copolymer, while maintaining consistently high yields. Their structures, along with the resulting copolymers, were confirmed using FT-IR, ^{1}H NMR and HPLC.

^{1}H NMR: ^{1}H NMR spectrum of monomeric 2,4-DMA (Fig. 1a) confirms the expected proton environments. Despite the limited resolution of the 60 MHz instrument, all characteristic signals were observed. A singlet at δ 2.080 ppm corresponds to the methyl protons. The non-equivalent methylene protons appear at δ 6.416 ppm (H_A) and δ 5.581 ppm (H_B), with H_A experiencing greater deshielding due to its proximity to the phenyl ring. Aromatic protons are observed in the δ 7.031-7.471 ppm range, showing a downfield shift relative to 2,4-dichlorophenol, consistent with the electron-withdrawing effect of the vinyl ester group. Integration values support the proton assignments and stoichiometric ratios within the ester structure.

^{1}H NMR spectrum of VMA monomer is presented in Fig. 1b. The characteristic monomeric resonances are observed at

TABLE-1
COPOLYMER COMPOSITION AND YIELD FOR LOW-CONVERSION RADICAL COPOLYMERIZATION OF 2,4-DMA AND VMA USING AIBN INITIATOR AT 70 ºC

Sample code No.	Monomer feed composition				Composition of 2,4-DMA in copolymer	Yield (%)
	2,4-DMA		VMA			
	Mole	Wt.%	Mole	Wt.%		
B-1	1.0	100	–	–	100	88
B-2	0.2	20	0.8	80	31.59	81
B-3	0.4	40	0.6	60	53.64	86
B-4	0.5	50	0.5	50	65.71	83
B-5	0.6	60	0.4	40	76.11	78
B-6	0.8	80	0.2	20	93.56	80
B-7	–	–	1.0	100	–	85

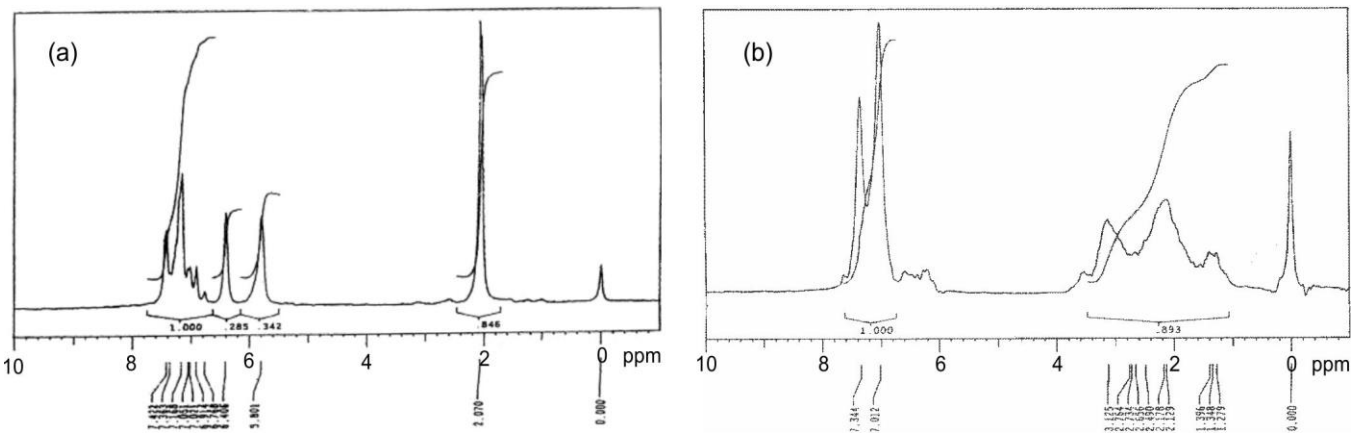

Fig. 1. ^{1}H NMR spectrum of (a) 2,4-DMA monomer and (b) VMA monomer

δ 5.931 ppm (1H, vinyl –CH=), δ 6.307 ppm (non-equivalent methylene, 1H) and δ 7.392-7.583 ppm (aromatic protons, 3H). Successful polymerization is confirmed by (i) disappearance of the vinyl proton signals (δ 5.931 and 6.307 ppm); (ii) emergence of broad signals at δ 3.125 ppm (methine proton, 1H) and δ 2.736-2.894 ppm (methylene protons, 2H), and (iii) slight upfield shifts of aromatic protons to δ 7.315-7.515 ppm, indicating changes in the electronic environment upon polymer formation.

FT-IR: The IR spectrum of 2,4-DMA monomer (Fig. 2a) exhibits characteristic absorption bands corresponding to its functional groups. Aromatic C–H stretching vibrations appear at 3106 cm^{-1}, while aliphatic C–H stretches are observed at 2980 cm^{-1} and 2850 cm^{-1}, with these bands remaining largely unchanged in the homopolymer spectrum. The vinyl C=C stretching vibration produces a distinct peak at 1640 cm^{-1}, complemented by a characteristic C–H out-of-plane bending mode of the vinyl group at 970 cm^{-1}. The spectrum reveals asymmetric CH_3 bending and CH_2 deformation vibrations at 1450 cm^{-1}, with symmetric CH_3 bending appearing at 1400 cm^{-1}. A strong carbonyl stretching at 1762 cm^{-1} confirms the ester functionality, while C–O stretching vibrations contribute to bands at 1217 cm^{-1}, 1247 cm^{-1} and 1089 cm^{-1}. Aromatic C–H out-of-plane bending vibrations appear at 805 cm^{-1} and 871 cm^{-1}, with C-Cl stretching vibrations producing a medium intensity band at 675 cm^{-1}. The FT-IR spectrum of poly(2,4-DMA) shows the characteristic absorption bands corresponding to aliphatic C–H stretching vibrations at 2980 cm^{-1} and 2850 cm^{-1}, demonstrating the minimal spectral shifts relative to the monomeric form. Remarkably, the diagnostic C=C stretching vibration at 1640 cm^{-1}, prominent in the monomer spectrum, undergoes complete disappearance upon polymerization, confirming the consumption of vinyl groups during the chain propagation. Similarly, the characteristic out-of-plane C–H deformation mode of the vinyl moiety at 970 cm^{-1} is conspicuously absent in the polymer spectrum, providing further spectroscopic evidence for the complete incorporation of double bonds into the polymeric backbone.

The vibrational spectrum of VMA monomer exhibits the characteristic infrared absorptions corresponding to its molecular structure as shown in Fig. 2b. The aromatic C–H stretching vibration appears at 3024 cm^{-1}, while aldehyde C–H stretches were observed at 2747 cm^{-1} and 2841.83 cm^{-1}. The carbonyl stretching frequency of the ester group produces a strong band at 1691 cm^{-1}. Aromatic C=C skeletal vibrations are evidenced by multiple absorptions at 1596, 1506.75 and 1460.62 cm^{-1}. The asymmetric and symmetric stretching modes of the C–O–C linkage appear at 1273 and 1207 cm^{-1} respectively. Key bands include (i) vinyl C–H out-of-plane deformation at 890 cm^{-1} and (ii) a characteristic absorption at 733.87 cm^{-1} confirming the *ortho*-disubstituted benzene ring configuration. The infrared spectrum of poly-VMA confirms its successful polymerization and structural features. Key evidence for polymerization includes the complete disappearance of the monomer's vinyl C–H bending vibration at 953 cm^{-1} and the C=C stretch at 1634 cm^{-1}. The spectrum verifies the presence of an *ortho*-disubstituted benzene ring indicated by a sharp peak at 732 cm^{-1} and supported by phenyl

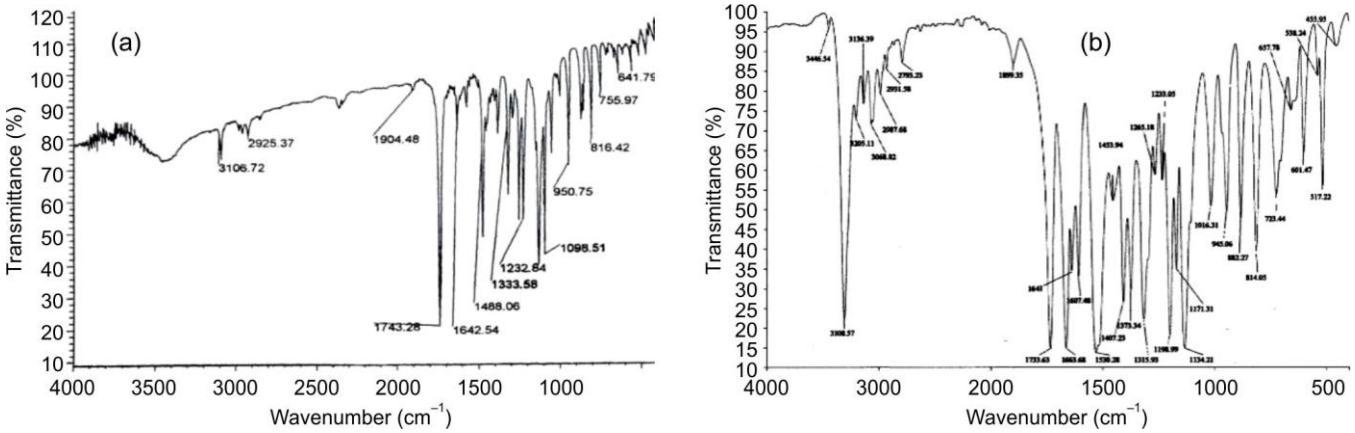

Fig. 2. FT-IR spectrum of (a) 2,4-DMA monomer and (b) VMA monomer

ring absorptions at 1597, 1503 and 1465 cm^{-1}. Carbonyl functionalities are confirmed by a prominent C=O stretch at ~1735-1702 cm^{-1} (comprising overlapping aldehyde and ketone/ester groups) and aldehyde-specific C–H stretches at 2849 and 2736 cm^{-1}. The preservation of the methoxy group is evidenced by a C–O–C bending mode at 1270 cm^{-1} and methyl deformation modes at 1390 and 1465 cm^{-1}. The gradual decrease in carbonyl band intensity with decreasing VMA content in the copolymers provides additional evidence for their compositional variation.

The absorption spectrum of poly(2,4-DMA-*co*-VMA) copolymer exhibits distinct vibrational features indicative of its compositional characteristics. A prominent absorption band at 1735 cm^{-1} arises primarily from the ester-carbonyl (C=O) stretching vibration, with a potential minor contribution from ketonic groups. Notably, the relative intensity of this band exhibits a systematic reduction correlating with decreased VMA incorporation in the copolymer series. Other key bands include (i) a well-defined absorption at 1390 cm^{-1}, characteristic of methyl group deformations and (ii) a strong vibrational mode at 1465 cm^{-1}, attributable to the asymmetric bending vibrations of methyl groups. These spectral features collectively provide compelling evidence for the successful formation of the copolymer structure with composition-dependent vibrational characteristics.

HPLC analysis: The chromatographic purity of the synthesized monomers was evaluated using HPLC analysis. The chromatogram of 2,4-DMA exhibited a single dominant peak, indicating a high purity of approximately 99%, confirming the successful preparation of the target ester with minimal impurities. Similarly, the VMA monomer displayed a singular dominant peak with an integrated area corresponding to 99.86% purity, demonstrating that the synthetic and purification procedures were highly effective. These results collectively verify the high polymer integrity and reproducibility of the synthesized monomers.

Biocidal efficacy: The synthesized acrylic copolymer of VMA and 2,4-DMA were evaluated against bacterial strains including *B. megaterium*, *E. coli*, *E. faecium* and *Salmonella*. The antimicrobial efficacy of the synthesized copolymers was found to be composition-dependent. For bacterial strains, the VMA homopolymer restricted *B. megaterium* growth to 55% of the polymer-free control, whereas 2,4-DMA homopolymer was more potent, limiting growth to 25%. Copolymers poly(VMA-*co*-2,4-DMA) exhibited intermediate activity, permitting 20-45% growth depending on the monomer ratio (Fig. 3a). In fungal assays, Fig. 3b show a clear dose-dependent inhibition of *A. niger* and *A. flavus* by VMA and 2,4-DMA, consistent with the strong antifungal effects observed in the assays. VMA homopolymer already suppresses *A. niger* growth to 58% of the control, while the copolymers further enhance inhibition (25-60% growth). The superior antimicrobial performance of chlorine-substituted 2,4-DMA copolymers aligns with their enhanced activity in the plots, likely due to the presence of 2,4-dichlorophenyl groups that strengthen antifungal efficacy, making these materials promising for applications requiring sustained microbial protection.

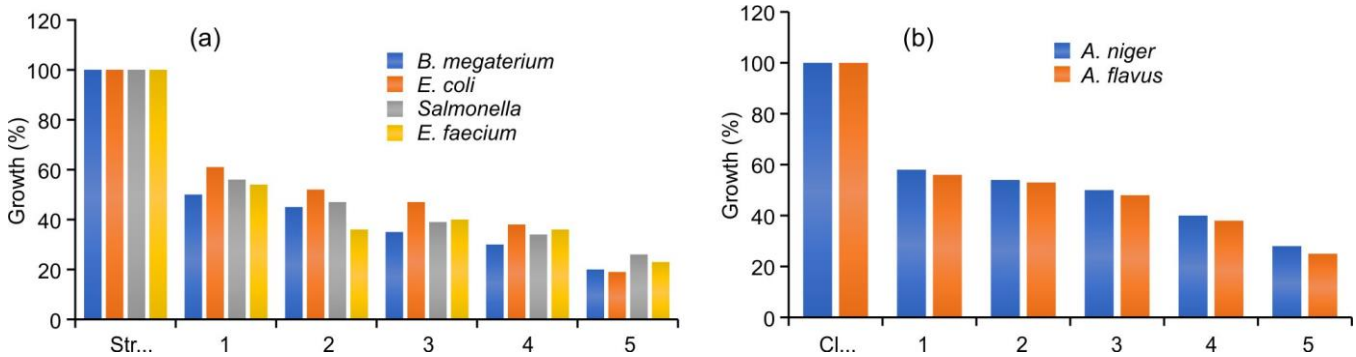

Fig. 3. Effect of VMA and 2,4-DMA on the growth (%) of bacteria (a) and fungi (b)

Molecular docking: Based on *in vitro* antibacterial screening, the most active compound was subjected to molecular docking analysis with DNA gyrase (PDB ID: 1KZN) to evaluate its binding interactions and affinity. The compound demonstrates a substantial interaction with DNA gyrase, exhibiting a binding affinity of −5.205 kcal/mol (Fig. 4). A conventional hydrogen bond was detected, characterized by a bond distance of 3.23 Å between the carbonyl oxygen of the ligand and the protein amino acid ASN46. Visual analysis suggests that the pi-alkyl interactions of the phenyl ring with amino acids ALA47 enhance the protein binding, with bond distances of 4.58 Å. Additionally, there is one pi-sigma interaction between the ligand's phenyl ring and the amino acid THR165, with a bond distance of 3.68 Å, along with two alkyl interactions of the chlorine atom in the ligand with amino acids VAL43 and VAL167, exhibiting bond distances of 3.69 Å and 4.50 Å, respectively.

Conclusion

A novel vinyl acrylic copolymer comprising 2,4-dichlorophenyl methacrylate (2,4-DMA) and vanillin methacrylate (VMA) was successfully synthesized *via* controlled radical polymerization. Comprehensive characterization using FT-IR, ^{1}H NMR and HPLC confirmed the structural integrity, high purity and reproducibility of the monomers and their copolymers. The copolymers exhibited composition-dependent antimicrobial activity against both bacterial and fungal strains, with chlorine-substituted 2,4-DMA units enhancing the biocidal efficacy. Molecular docking studies supported these findings, revealing strong interactions of the copolymer component with DNA gyrase (PDB ID: 1KZN), which is consistent with its observed antibacterial activity. Overall, the study demonstrates that these copolymers possess significant potential for applications requiring sustained antimicrobial protection, including biomedical materials, coatings and packaging.

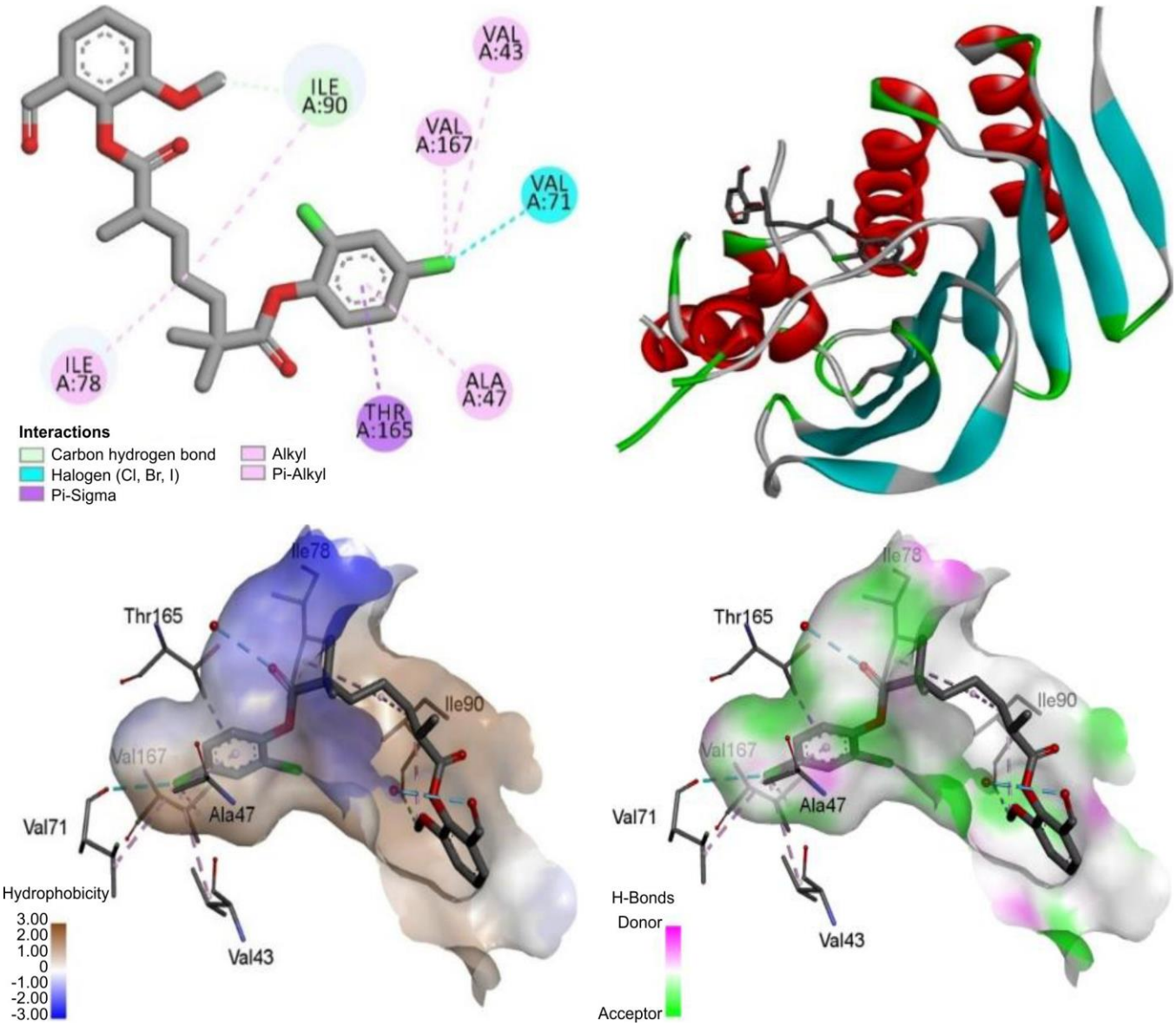

Fig. 4. Molecular docking assessment of methacrylate copolymers

ACKNOWLEDGEMENTS

The authors gratefully acknowledge the Department of Chemistry, Sardar Patel University, Vallabh Vidyanagar for providing the necessary research infrastructure and facilities for the synthesis and characterization of acrylic copolymer. Lastly, the authors acknowledge the efforts of all colleagues and supporting staff who contributed their time and effort to ensure the smooth progress of this study.

CONFLICT OF INTEREST

The authors declare that there is no conflict of interests regarding the publication of this article.

DECLARATION OF AI-ASSISTED TECHNOLOGIES

During the preparation of this manuscript, the authors used an AI-assisted tool(s) to improve the language. The authors reviewed and edited the content and take full responsibility for the published work.

REFERENCES

1. D. Silvestri, M. Gagliardi, N. Barbani, C. Cristallini and P. Giusti, *Drug Deliv.*, **16**, 116 (2009); https://doi.org/10.1080/10717540802666980
2. L.-C. Wang, X.-G. Chen, D.-Y. Zhong and Q.-C. Xu, *J. Mater. Sci. Mater. Med.*, **18**, 1125 (2007); https://doi.org/10.1007/s10856-007-0159-5
3. R.V. Gadhave, *Open J. Polym. Chem.*, **13**, 1 (2023); https://doi.org/10.4236/ojpchem.2023.131001
4. J.P.K. Tan, C.H. Goh and K.C. Tam, *Eur. J. Pharm. Sci.*, **32**, 340 (2007); https://doi.org/10.1016/j.ejps.2007.08.010
5. U. Senthilkumar, R. Balaji and S. Nanjundan, *J. Appl. Polym. Sci.*, **81**, 96 (2001); https://doi.org/10.1002/app.1418
6. U. Senthilkumar, K. Ganesan and B.S.R. Reddy, *J. Polym. Res.*, **10**, 21 (2003); https://doi.org/10.1023/A:1023938301946
7. S. Thamizharasi, G. Srinivas, N. Sulochana and B.S.R. Reddy, *J. Appl. Polym. Sci.*, **73**, 1153 (1999); https://doi.org/10.1002/(SICI)1097-4628(19990815)73:7<1153::AID-APP7>3.0.CO;2-D
8. X. Zhang, M. Du, H. Fang, M. Shi, C. Zhang and F. Wang, *Constr. Build. Mater.*, **299**, 124290 (2021); https://doi.org/10.1016/j.conbuildmat.2021.124290
9. M. Matamoros-Ambrocio, E. Sánchez-Mora, E. Gómez-Barojas and J.A. Luna-López, *Polymers*, **13**, 2171 (2021); https://doi.org/10.3390/polym13132171
10. S. Mushtaq, N.M. Ahmad, A. Mahmood and M. Iqbal, *Polymers*, **13**, 216 (2021); https://doi.org/10.3390/polym13020216
11. T.K. Murtadha, *Results Eng.*, **17**, 100875 (2023); https://doi.org/10.1016/j.rineng.2023.100875
12. P.R. Raja, *Rev. Adhesion Adhesives*, **4**, 398 (2016); https://doi.org/10.7569/RAA.2016.097315
13. Z. Tang and S. Li, *Curr. Opin. Solid State Mater. Sci.*, **18**, 119 (2014); https://doi.org/10.1016/j.cossms.2014.02.002
14. A. Martini, U.S. Ramasamy and M. Len, *Tribol. Lett.*, **66**, 58 (2018); https://doi.org/10.1007/s11249-018-1007-0
15. J. Lomège, V. Mohring, V. Lapinte, C. Negrell, J.-J. Robin, and S. Caillol, *Eur. Polym. J.*, **109**, 435 (2018); https://doi.org/10.1016/j.eurpolymj.2018.10.015
16. I. Minami, *Appl. Sci.*, **7**, 445 (2017); https://doi.org/10.3390/app7050445
17. K. Pieters and T.H. Mekonnen, *RSC Sustain.*, **2**, 3704(2024); https://doi.org/10.1039/d4su00267a
18. N.P. Badgujar, R.D. Kulkarni, C. Govindasamy, H.V. Patil, M.L. Bari and K. Nagaraj, *J. Indian Chem. Soc.*, **101**, 101372 (2024); https://doi.org/10.1016/j.jics.2024.101372
19. J. Solera-Sendra, N. Ballard, L.J. del Valle and L. Franco, *Polymers*, **17**, 1027 (2025); https://doi.org/10.3390/polym17081027
20. B.M. Rosales, A.R. Di Sarli, O. De Rincón, A. Rincón, C.I. Elsner and B. Marchisio, *Prog. Org. Coat.*, **50**, 105 (2004); https://doi.org/10.1016/j.porgcoat.2003.12.002
21. N. Siyab, S. Tenbusch, S. Willis, C. Lowe and J. Maxted, *J. Coat. Technol. Res.*, **13**, 629 (2016); https://doi.org/10.1007/s11998-015-9766-0
22. P.S. Vijayanand, S. Kato, S. Satokawa and T. Kojima, *J. Appl. Polym. Sci.*, **108**, 1523 (2008); https://doi.org/10.1002/app.27319
23. A.V. Singh, A. Rahman, N.V.G. Sudhir Kumar, A.S. Aditi, M. Galluzzi, S. Bovio, S. Barozzi, E. Montani and D. Parazzoli, *Mater. Des.*, **36**, 829 (2012); https://doi.org/10.1016/j.matdes.2011.01.061.
24. J. Ghosh, N.S. Rupanty, T. Noor, T.R. Asif, T. Islam and V. Reukov, *RSC Adv.*, **15**, 10984 (2025); https://doi.org/10.1039/D5RA01429H
25. W. Ye, M.F. Leung, J. Xin, T.L. Kwong, D.K.L. Lee and P. Li, *Polymer*, **46**, 10538 (2005); https://doi.org/10.1016/j.polymer.2005.08.019
26. R.P. Rosa, G. Rosace and V. Trovato, *Polymers*, **16**, 2111 (2024); https://doi.org/10.3390/polym16152111
27. A.R. Banks, R.F. Fibiger and T. Jones, *J. Org. Chem.*, **42**, 3965 (1977); https://doi.org/10.1021/jo00444a042
28. S. Hadiouch, M. Maresca, D. Gigmes, G. Machado, A. Maurel-Pantel, S. Frik, J. Saunier, A. Deniset-Besseau, N. Yagoubi, L. Michalek, C. Barner-Kowollik, Y. Guillaneuf and C. Lefay, *Polym. Chem.*, **13**, 69 (2022); https://doi.org/10.1039/D1PY01344K
29. I. Asnawi, E. Febrina, W. Aligita, L. O. Aman and F. Razi, *J. Pharm. Pharmacogn. Res.*, **12**, 822 (2024); https://doi.org/10.56499/jppres23.1926_12.5.822
30. E. Kenawy, A.R. Ghazy, A.F. Al-Hossainy, M. Bishr and M.M. Azzam, *Environ. Sci. Pollut. Res.*, **30**, 109250 (2023); https://doi.org/10.1007/s11356-023-30043-4